ELSEVIER

Journal of Power Sources 54 (1995) 508–510

JOURNAL OF POWER SOURCES

Amorphous MoS_2 as the cathode of lithium secondary batteries

Yasuhiro Miki, Daisuke Nakazato, Hiromasa Ikuta, Takashi Uchida, Masataka Wakihara

Department of Chemical Engineering, Tokyo Institute of Technology, Ookayama, Meguro-ku, Tokyo 152, Japan

Abstract

Amorphous MoS_2(a-MoS_2) was synthesized by the thermal decomposition of $(NH_4)_2MoS_4$ in a hydrogen gas flow at temperatures from 150 to 300 °C. The a-MoS_2 synthesized at 150 and 200 °C were almost amorphous. However, those prepared at 250 and 300 °C showed very small and broad peaks in powder X-ray diffraction patterns. Discharge/charge cycling measurements, revealed that the sample prepared at 150 °C showed the highest cycle capacity (100 Ah/kg) at the 100th cycle. The chemical diffusion coefficients of lithium were also highest for a-MoS_2 prepared at 150 °C, and the $\tilde{D}$ values fell in the range of $-10 < \log(\tilde{D}/cm^2\ s^{-1}) < -9$.

Keywords: Secondary lithium batteries; Molybdenum sulfide; Cathodes

1. Introduction

Lithium secondary cells using MoS_2 have attracted attention for many years and these cells were once commercialized as the first practical lithium rechargeable batteries [1]. Crystalline MoS_2 has been mainly used in the studies. However, it is well known that amorphous compounds sometimes show better properties as the cathode and/or anode than the crystalline compounds of the same materials in lithium secondary cells [2], because amorphous compounds with low densities usually have a wider space for Li^+ diffusion. Furthermore, the disappearance of a long range order in amorphous compounds leads to the improvement of their cycle life. Accçording, it is worthwhile to investigate the cathode properties of a-MoS_2.

When $(NH_4)_2MoS_4$ is thermally decomposed in an inert atmosphere (e.g., in argon) at about 300 °C, a-MoS_3 forms [3]. However, a-MoS_2 can be prepared when it is decomposed in an hydrogen atmosphere at temperatures lower than 300 °C [4].

On the other hand, the chemical diffusion coefficient of lithium is one of the most important factors to evaluate its cathode or anode properties. Several methods have been proposed to derive the chemical diffusion coefficient of lithium in the electrodes in lithium secondary cells, for example, current-pulse relaxation method [5], potential step chronoamperometry (PSCA) [6–8], a.c. impedance method [9] and galvanostatic intermittent titration technique [10].

In this study, several types of a-MoS_2 are prepared by the thermal decomposition of $(NH_4)_2MoS_4$ in hydrogen atmosphere at temperatures from 150 to 300 °C. The cathode properties of these a-MoS_2 compounds, such as discharge profiles, cyclic voltammograms, discharge/charge cycle lives, are measured. The chemical diffusion coefficient of lithium in these materials is also estimated.

2. Experimental

Various a-MoS_2 compounds were synthesized by the thermal decomposition of $(NH_4)_2MoS_4$ in an hydrogen gas flow at temperatures of 150, 200, 250 and 300 °C. The samples were characterized by powder X-ray diffraction (XRD) method (Cu Kα, Rigaku, Rotaflex RU-200). The electrical conductivities of a-MoS_2 were measured by a d.c. two-electrode method.

A mixture of a-MoS_2, acetylene black, and polytetrafluoroethylene in the ratio of 70:20:10 in wt.% was pressed into a film of 0.1 mm thick. Discs of 5 mm in diameter (2–3 mg) were cut from the film then used as the cathode. Excess amount of lithium foil (1 mm thick) was used as the anode. 1 M $LiClO_4$ dissolved in propylene carbonate (PC) (Tomiyama Pure Chemical Industries, Ltd.) was used as the electrolyte. Galvanostatic discharge/charge cycling tests were carried out under a current density of 0.5 mA/cm^2 at cutoff voltages

SSDI 0378-7753(94)02136-Q

between 1 and 3 V. Cyclic voltammograms were obtained under a sweep rate of 1.5 mV/cm in the range from 1 to 3 V.

The open-circuit voltages (OCV) of the Li|a-MoS_2 cells were measured as follows. A cell was discharged to a desired lithium content, then the cell was left with the electric circuit open until the cell voltage became stable. The final voltage was observed as the OCV at that composition.

Chemical diffusion coefficients of lithium, $\tilde{D}$ (cm^2/s), were measured by the current pulse relaxation method. $\tilde{D}$ values are calculated from the following equation:

$$\tilde{D} = \frac{1}{\pi}\left(\frac{V_M(dE/dx)}{nFa}\frac{i\tau}{m_D}\right)^2 \quad (1)$$

where V_M is the electrode molar volume of MoS_2 (cm^3), dE/dx the OCV gradient, n the change of lithium ($n=1$), F the Faraday constant, a the electrode surface area (cm^2), i the pulse current (mA), τ the pulse duration (s), m_D the slope of the ΔE versus $1/\sqrt{t}$ (t = relaxation time) plot (V $s^{-1/2}$). The current and the duration of the pulse were 0.114 mA and 10 s, respectively. The geometrical electrode surface area ($a=0.229$ cm^2) and the theoretical molar volume of crystalline MoS_2 ($V_M=32$ cm^3) were used for the calculation.

All the electrochemical measurements were carried out by using two-electrode cells in an argon-filled glove box.

3. Results and discussion

XRD patterns for a-MoS_2 are shown in Fig. 1. a-MoS_2 synthesized at 300 °C (a-MoS_2(300)) and at 250 °C (a-MoS_2(250)) showed a few very small and broad peaks (at $2\theta=14°$, 33° and 58°). Therefore, a-MoS_2(300) and a-MoS_2(250) are slightly crystallizing. On the other hand, a-MoS_2(200) and a-MoS_2(150) were almost amorphous because they showed no peaks. From the XRDpeaks of (002) ($2\theta=14°$) and (110) ($2\theta=58°$) for a-MoS_2(250), the crystallite size was estimated to be $L_a=5.3$ nm and $L_c=5.7$ nm using Scherrer's equation [11]. The electrical conductivities of a-MoS_2 are given in Table 1 . Those of crystalline MoS_2 is also shown for comparison. The conductivities of a-MoS_2 were greater than that of crystalline MoS_2.

The first discharge curves of the Li|a-MoS_2 cells are shown in Fig. 2. The discharge capacity was the highest

Table 1
Electrical conductivity for amorphous and crystalline MoS_2

	Amorphous MoS_2			Crystalline MoS_2
	150 °C	200 °C	250 °C	
σ (S m^{-1})	2.66×10^{-4}	1.09×10^{-3}	1.45×10^{-3}	2.52×10^{-6}

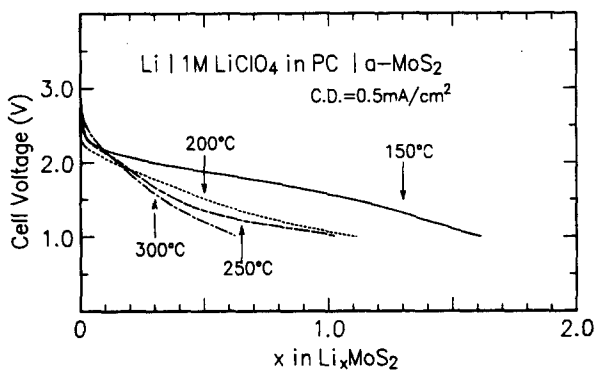

Fig. 2. The first discharge curves for Li|a-MoS_2 cells.

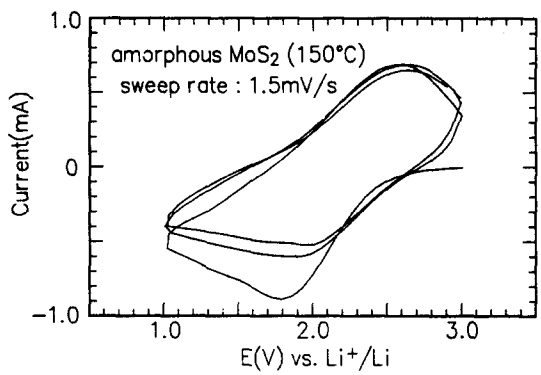

Fig. 3. Cyclic voltammogram of a Li|a-MoS_2(150) cell.

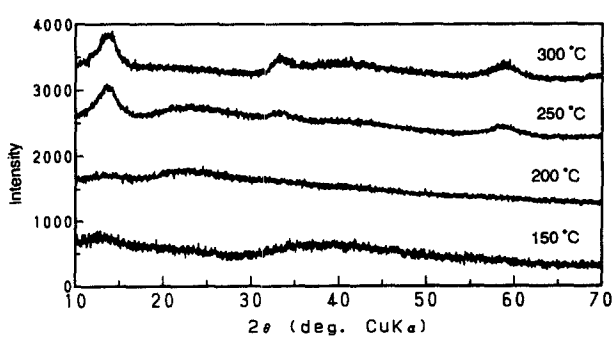

Fig. 1. X-ray diffraction patterns of amorphous MoS_2.

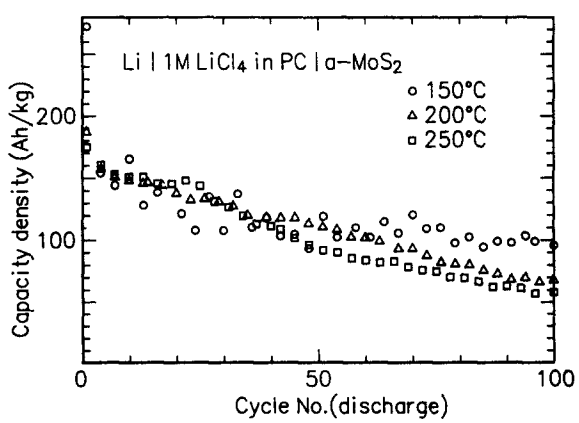

Fig. 4. Cycling properties of Li|a-MoS_2 cells.

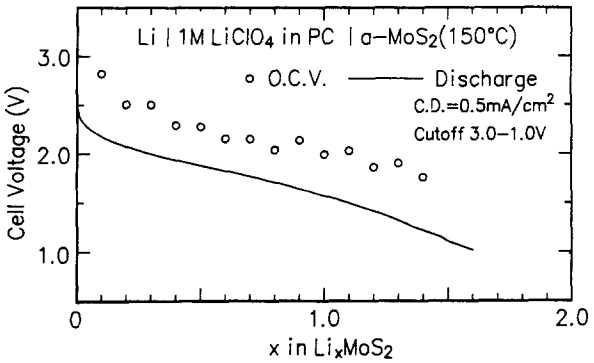

Fig. 5. Compositional variation of open-circuit voltage in the Li|a-MoS_2(150) cell. The first discharge curve is also shown.

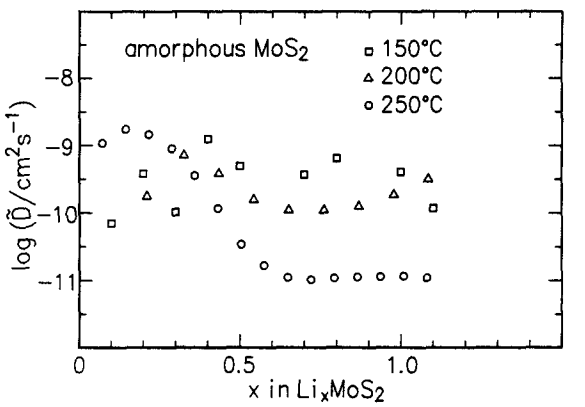

Fig. 6. Chemical diffusion coefficients of lithium vs. x in Li_xMoS_2.

for the a-MoS_2(150), and it decreased when the preparation (decomposition) temperature increased (a-MoS_2(200) > a-MoS_2(250) > a-MoS_2(300)). The discharge voltage of the Li|a-MoS_2(150) cell was also the highest among the four types of Li|a-MoS_2 cells. It is known that the discharge curve of the Li|crystalline-MoS_2 cell has a plateau at about 1.1 V where the coordination of Mo by six S atoms (MoS_6) changes from trigonal prismatic to octahedral in the MoS_2 structure while lithium ions intercalate into MoS_2 [12]. The relatively flat region observed in the discharge curve of the Li|a-MoS_2(250) cell at voltages lower than 1.3 V ($x > 0.5$) correspond to this change in the MoS_6 coordination from trigonal prismatic to octahedral occurring in the small portion of crystalline MoS_2 (observed by XRD described above).

The cyclic voltammograms of the Li|a-MoS_2(150) cell for the initial three cycles is given in Fig. 3. The anodic peak at 1.8 V in the first cycle shifted to 2.0 V in the second and third cycles, while all the cathodic peaks appeared at the same voltage, indicating that the discharge/charge cycle of this cell is reversible as from the second cycle.

The results of the discharge/charge cycling tests of the lithium cells using a-MoS_2(150), a-MoS_2(200) and a-MoS_2(250) are shown in Fig. 4. Those of the a-MoS_2(300) cell were obviously inferior to those of the other cells. This Figure shows that the discharge capacities during the third cycle are almost comparable for all the three cells. Accordingly, the largest discharge capacity of the a-MoS_2(150) cell in the first cycle (Fig. 3) may be due to irreversible reactions (which are not clear at present). In the following cycles, the a-MoS_2(150) cell exhibited the highest discharge capacity among the three cells, which means that a-MoS_2(150) is the most favourable cathode material among these three compounds.

The typical compositional variation of the OCV, which was observed for the a-MoS_2(150) cell, are plotted in Fig. 5.

Chemical diffusion coefficients of lithium are shown in Fig. 6. The $\tilde{D}$ values observed for a-MoS_2(250) decreased with increasing lithium content up to $x = 0.6$, then it became constant at $\log \tilde{D} \simeq -11$. It is evident that the chemical diffusion coefficient decreases with increasing lithium content, because the coulombic repulsion of lithium ions increases. However, in the case of a-MoS_2(200) and a-MoS_2(150), the $\tilde{D}$ values were found to be almost constant in whole the range of x, indicating that the coulombic repulsion of lithium ions is smaller in a-MoS_2(150) and a-MoS_2(200) than in a-MoS_2(250). These results may suggest that a-MoS_2(150) and a-MoS(200) have a wider space for the diffusion of Li^+ ion than partially crystallized a-MoS_2(250). The $\tilde{D}$ values were slightly higher for a-MoS_2(150) than for a-MoS_2(200). These results may support the superiority of a-MoS_2(150) compared with the other compounds observed in the cylinder test.

References

[1] R.R. Haering, J.A.R. Stiles and K. Brandt, *US Patent No. 4 224 390* (1980).
[2] Y. Sakurai and J. Yamaki, *J. Electrochem. Soc., 132* (1985) 512.
[3] A.J. Jacobson, R.R. Chiannelli, S.M. Rich and M.S. Wittingham, *Mater. Res. Bull., 14* (1979) 379.
[4] T. Ozaki et al., *Ext. Abstr., 63rd Spring Meet. The Chemical Society of Japan, Osaka, Japan, 30 Mar. 1992,* p. 269.
[5] S. Basu and W. Worrel, in P. Vashishta, J.N. Mundy and G.K. Shenoy (eds.), *Fast Ion Transport in Solids,* Elsevier, Amsterdam, 1979, p. 149.
[6] K. Kanamura, K. Yuasa and Z. Takehara, *J. Power Sources, 20* (1987) 127.
[7] Z. Takehara, K. Kanamura, S. Yonezawa and T. Hanada, *J. Power Sources, 25* (1989) 1277.
[8] K. Kanamura, S. Yonezawa, S. Yoshioka and Z. Takehara, *J. Phys. Chem., 95* (1991) 7939.
[9] C. Ho, I.D. Raistrick and R.A. Huggins, *J. Electrochem. Soc., 127* (1980) 343.
[10] W. Weppner and R.A. Huggins, *J. Electrochem. Soc., 124* (1979) 1569.
[11] P. Scherrer, *Göttinger Nachr., 68* (1928).
[12] R. Haering, J.A.R. Stiles and K. Brandt, *US Patent No. 4 281 048* (1982).